Available online at www.sciencedirect.com

ScienceDirect

MATTER AND RADIATION AT EXTREMES

Matter and Radiation at Extremes 2 (2017) 243–255

www.journals.elsevier.com/matter-and-radiation-at-extremes

Review Article

Laser performance upgrade for precise ICF experiment in SG-III laser facility

Wanguo Zheng [a,b], Xiaofeng Wei [a], Qihua Zhu [a,b], Feng Jing [a], Dongxia Hu [a,b], Xiaodong Yuan [a], Wanjun Dai [a], Wei Zhou [a], Fang Wang [a], Dangpeng Xu [a], Xudong Xie [a], Bin Feng [a], Zhitao Peng [a], Liangfu Guo [a], Yuanbin Chen [a], Xiongjun Zhang [a], Lanqin Liu [a], Donghui Lin [a], Zhao Dang [a], Yong Xiang [a], Rui Zhang [a], Fang Wang [a], Huaiting Jia [a], Xuewei Deng [a,b,*]

[a] *Laser Fusion Research Center, China Academy of Engineering Physics, P.O. Box 919-988, Mianyang, 621900, China*
[b] *IFSA Collaborative Innovation Center, Shanghai Jiao Tong University, Shanghai, 200240, China*

Received 21 May 2017; revised 12 July 2017; accepted 21 July 2017
Available online 15 August 2017

Abstract

The SG-III laser facility (SG-III) is the largest laser driver for inertial confinement fusion (ICF) researches in China, which has 48 beamlines and can deliver 180 kJ ultraviolet laser energy in 3 ns. In order to meet the requirements of precise physics experiments, some new functionalities need to be added to SG-III and some intrinsic laser performances need upgrade. So at the end of SG-III's engineering construction, the 2-year laser performance upgrade project started. This paper will introduce the newly added functionalities and the latest laser performance of SG-III. With these function extensions and performance upgrade, SG-III is now fully prepared for precise ICF experiments and solidly paves the way towards fusion ignition.

PACS Codes: 52.57.-z; 42.60.-v; 42.55.-f; 28.52.-s

Keywords: Inertial confinement fusion; Laser driver; SG-III; Power balance; Beam smoothing

1. Introduction

Controllable nuclear fusion might be the most ambitious plan for human beings in the 21st century, by which people on the earth may completely overcome the forthcoming energy crisis [1]. Laser-driven inertial confinement fusion (ICF) is one of the major approaches to achieve this goal, and the first step is to realize fusion ignition [2], that means the fusion energy is equal to or a little bit higher than the drive one. Among the countries that make efforts on ICF researches, the U.S. fully deserves to be called a pioneer in exploring laser driven technologies and ICF physics. In the past half century, the U.S. had built a series of laser drivers such as the NOVA [3] and the OMEGA [4] laser facilities with 10 kJ level output energies to prepare laser technologies and understanding in ICF physics before the National Ignition Facility (NIF) [5] with MJ-level output energy was designed and built. However, it looks much more difficult to achieve ignition than expected. The National Ignition Campaign (NIC) [6] carried out in NIF failed to ignite [7] and achieving ignition on NIF remains "unlikely in the near-term (one or two years) and uncertain in the mid-term (five years)" [7]. Besides facilities in the U.S., there is another ignition-level laser driver under construction in the world – the Laser Megajoule (LMJ) [8] in France. It

* Corresponding author. Laser Fusion Research Center, China Academy of Engineering Physics, P.O. Box 919-988, Mianyang, 621900, China.
E-mail address: xwdeng@caep.cn (X.W. Deng).
Peer review under responsibility of Science and Technology Information Center, China Academy of Engineering Physics.

http://dx.doi.org/10.1016/j.mre.2017.07.004

was designed to provide 1.8 MJ ultraviolet laser energy by 240 laser beams. Its construction progress seems to slow down after the setbacks in NIC.

China has also been developing laser technologies for ICF researches since last century [9]. At present, there are three laser facilities working routinely for physics experiments – the SG-II laser facility in Shanghai [10], the SG-III prototype [11] and the SG-III laser facility in Mianyang [12]. Among the SG series laser facilities, SG-III is now the largest laser driver in China, whose engineering construction was finished in 2015, as shown in Fig. 1. SG-III processes 48 laser beamlines distributing in 6 bundles with 4 × 2 arrangement. The 1053 nm pulsed laser is generated in the front-end system, which is then temporally shaped, amplified to nanojoule level and propagates to the pre-amplifier system located in the laser hall. Here the laser is amplified again to Joule level and spatially shaped to a square shape. Then the laser pulse is injected into the main-amplifier system, where the laser pulse will pass the main amplifier 4 times and the power amplifier 3 times. The output 1053 nm laser energy is 7500 J with 360 mm × 360 mm beam size. The laser pulse is then switched in the switchyard and enters the target chamber through final optics assembly (FOA), in which the laser is converted to 351 nm (3ω) with 3750 J/1.25 TW and focused. The whole 48 laser beamlines can deliver 180 kJ ultraviolet laser energy onto target in 3 ns. This energy level is right between 10 kJ and MJ level laser facilities in the U.S., thus the physics problems arising during the extrapolation from 10 kJ to MJ can be further understood and help the physicists revise the physics design for achieving ignition. At this point of view, SG-III is an important platform for China that suits resolved experiments for better understanding of some specific physics processes in the hohlraum and the extrapolation problems before laser energy reaching MJ level, such as the laser plasma interactions (LPI) [13] and implosion symmetry tuning [14].

In order to meet the requirements of precise physics experiment, such as probing lasers for LPI and Thomson scattering (TS), time fiducial for diagnostics, more precise laser control capabilities, a two-year performance upgrade project in SG-III was started in 2014. Some new functionalities were added, such as the beamline for LPI and TS, laser source for time fiducial and velocity interferometer system for any reflector (VISAR), and wavelength tuning. What is more important, two key laser control capabilities have been obviously improved after this project – the power balance and the beam smoothing capabilities. These two laser capabilities are most concerned in physics experiments since they directly influence the implosion symmetry [15] and the increasing of LPI instability [13]. In this paper, we briefly review the function extensions and make a comprehensive introduction of the SG-III laser performance upgrade including power balance and beam smoothing, after which the capabilities for precise physics experiments of SG-III has been improved significantly.

2. New functionalities added to SG-III

To extend SG-III's experiment capability, some new functionalities are added to the facility, including beamline for LPI and TS probing, laser source for time fiducial and VISAR, and wavelength tuning.

2.1. Beamline for LPI and TS probing

When intense lasers shoot on the hohlraum wall, plasmas expand quickly, and then LPI can induce strong back scattering like stimulated Raman scattering (SRS) and stimulated Brillouin scattering (SBS), which cause laser energy loss and asymmetrical pellet implosions [16]. For better understanding of the LPI process and plasma conditions in the hohlraum, a new beamline that can provide 3ω laser for LPI and 4ω laser for TS probing is required to be added, as shown in Fig. 2.

This beamline is selected from the original beamlines of SG-III and redirected to the north pole (top) of the target chamber, as shown in Fig. 3. When the switch mirror is

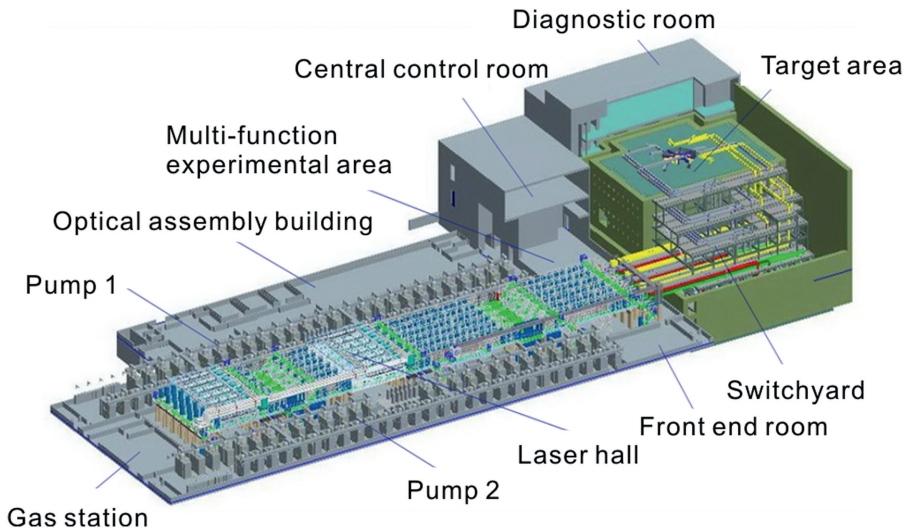

Fig. 1. The architecture of SG-III.

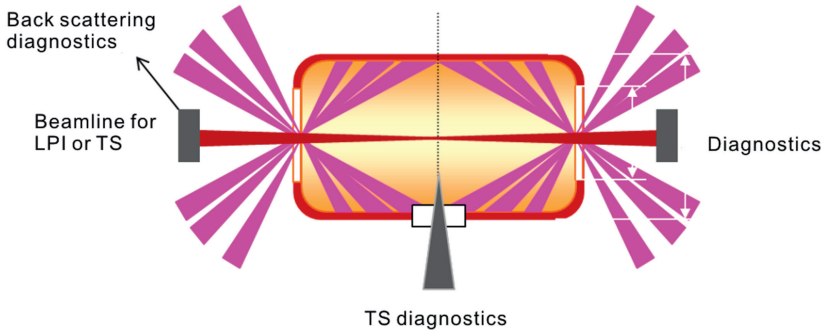

Fig. 2. Schematic of the beamline for LPI and TS.

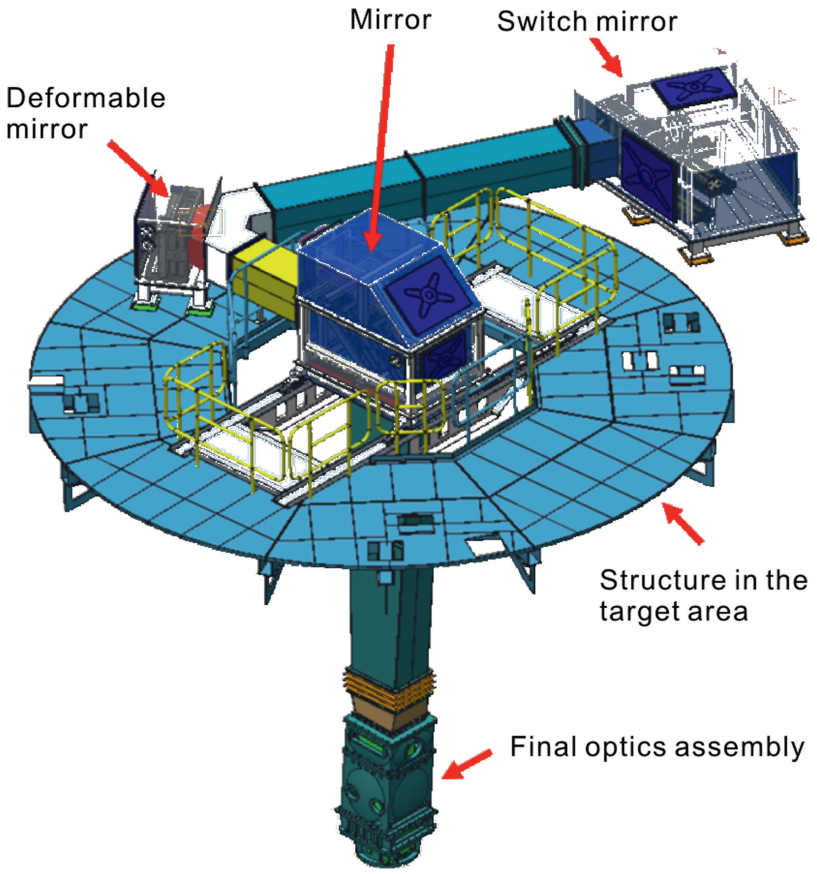

Fig. 3. LPI and TS beamline is located at the top of the target chamber.

inserted into the beam path, the laser is directed to its original position at the inner ring of the chamber and when the switch mirror is moved off, this laser beam is redirected to the north pole, wavefront-corrected by a deformable mirror, and finally frequency-tripled and focused into the hohlraum by an final optics assembly (FOA). Here, two different FOAs are designed and fabricated for the 3ω LPI laser and 4ω TS probing laser respectively. The FOA for 3ω LPI laser is newly fabricated but as same as the original ones in SG-III, in which the square beam size is still 360 mm $\times$ 360 mm. Typical testing data of this 3ω LPI beamline are: laser energy 3804 J, flat-top pulse with duration 2.97 ns and bandwidth 0.12 nm, 95% laser energy encircled in a 378 μm-diameter circle, power density on target 1.14×10^{15} W/cm^2.

The FOA for the 4ω TS probing laser is newly designed and quite different from the previous FOAs in SG-III. The 4ω laser is generated by a 2-step type-I second harmonic generation process. First, the fundamental laser is frequency doubled by a KDP crystal with 16 mm thickness; Second, the 2ω laser is again frequency doubled by another KDP crystal with 7 mm thickness. Since the requirement for 4ω laser energy is 300 J, the beam size of the 4ω laser is limited to Φ180 mm. A temperature controller is used with 0.1 °C precision during the 4ω generation process due to its temperature sensitivity. A lens with 1.7 m focal length is placed in the target chamber to focus the 4ω laser into the hohlraum, and its back surface is used to sample a little part of the 4ω laser into a diagnostic package. The FOA design is shown in Fig. 4. In order to separate the left

1ω and 2ω lasers, the center of the beam nearfield is sheltered and only the 4ω laser can inject into the hohlraum. In our test of this 4ω beamline, the flat-top 3 ns 4ω laser energy is 379 J. The X-ray focal spot at high laser power density captured by a pinhole camera is shown in Fig. 5(a), and the optical focal spot at very low laser power density captured by a CCD camera is shown in Fig. 5(b).

2.2. Laser source for time fiducial and VISAR

During ICF experiments, different diagnostic devices are involved to provide detailed information of the physics process, for example, the streak camera, framing camera, Dante and so on. It is quite important to relate different incidents from different devices together with laser driven by a time fiducial. Thus it is essential to provide a time fiducial signal to diagnostic devices. In our performance upgrade project, a laser source providing precise optical time fiducial is required to be added to SG-III. Fig. 6 shows the system design for this time fiducial laser source and Fig. 7 is a picture of the time fiducial system and VISAR table as currently installed in SG-III. A 1064 nm distributed feedback (DFB) fiber laser source is used to generate the continuous-wave (CW) laser, which is shaped to a pulse train (typically 10 pulses) by an amplitude modulator. This pulse train is then amplified by a series of fiber and rod amplifiers, frequency converted and split to multiple output channels. The energy of the 532 nm or 355 nm single pulse in the pulse train is over 0.1 mJ, and the pulse width (FWHM) is about 80 ps with pulse separation tunable in integer time of 100 ps. The performance of this time fiducial laser source has been demonstrated in physics experiments. Fig. 8 shows X-ray signals of the time fiducial laser pulse train which is captured by a streak camera. These time fiducial signals provide precise time reference for physics incidents.

Measurements of shock waves in ICF experiments possess the characteristics of small scale, ultrahigh pressure, ultrahigh speed, ultrashort duration and ultrahigh time resolution. In this area, VISAR is a major technique and widely used [17,18]. The VISAR measurement in SG-III requires a laser source that provides flat-top laser pulses at 532 nm, single pulse energy more than 20 mJ and pulse duration larger than 20 ns. These laser requirements can be met by simply changing the time fiducial laser system as shown in Figs. 6 and 7. By increasing the pump voltage of the rod amplifier unit, a 20 mJ/20 ns flat-top pulse can be delivered at the output. This laser source meets all the requirements in physics experiments, providing reliable support to obtain the physics images of shock loading and velocity slowing down. Fig. 9 shows the shock wave velocity of a quartz sample measured in SG-III with the imaging VISAR system using this laser source.

2.3. Wavelength tuning

Before ignition target design, it is very important to understand the basic physics laws of the LPI processes. It is demonstrated in NIC that when one slightly changes the laser central wavelengths among different driven rings, the cross-

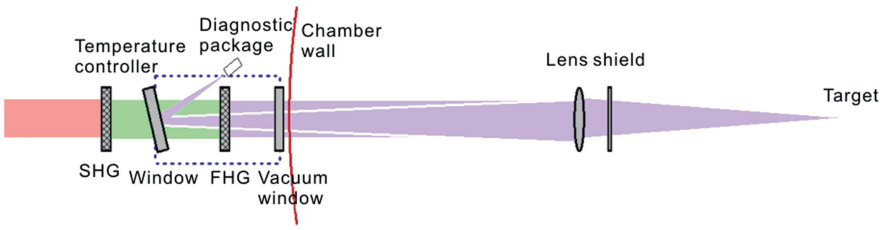

Fig. 4. The FOA design for the 4ω TS probing laser. Legend: SHG: second harmonic generator, FHG: fourth harmonic generator.

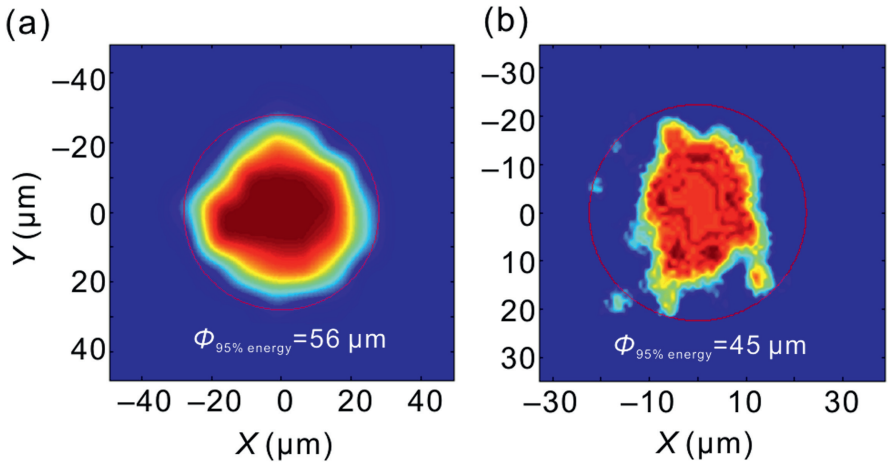

Fig. 5. (a) The X-ray focal spot at a high 4ω laser power density captured by the pinhole camera; and (b) the optical focal spot at a very low laser power density captured by the CCD camera.

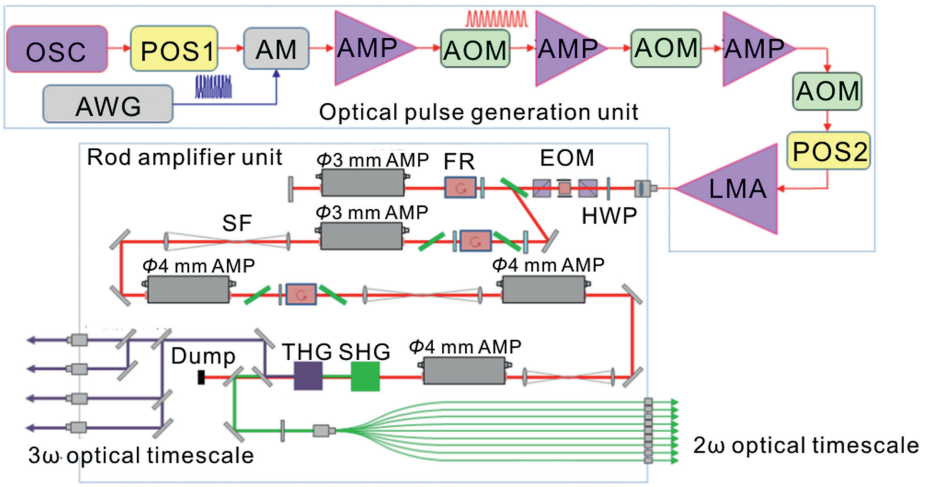

Fig. 6. Design of the laser system for SG-III's time fiducial. Legend: OSC: oscillator, POS: polarization stabilizer, AM: amplitude modulator, AMP: amplifier, AOM: acoustic optical modulator, LMA: large mode area amplifier, HWP: half wave plate, EOM: electro-optical modulator, FR: Faraday rotator, SF: spatial filter, SHG: second harmonic generator, THG: third harmonic generator.

Fig. 7. The laser system for time fiducial and VISAR in SG-III.

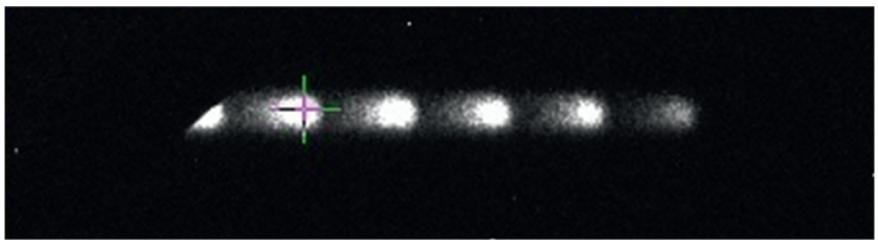

Fig. 8. The 355 nm time fiducial signals captured by an X-ray streak camera.

beam energy transfer occurs, which can mitigate the energy loss in the inner ring and optimize the implosion symmetry [19]. In order to study cross-beam energy transfer and mitigate the energy loss by LPI, it is required to realize wavelength tuning in one beamline of SG-III. Two DFB fiber laser sources with central wavelengths at 1052.7 nm and 1053.3 nm respectively and tuning range ±0.35 nm are used to provide a total tuning range from 1052.5 nm to 1053.5 nm with 0.1 nm tuning precision. A 2 × 1 optical switch is used to select the proper DFB laser according to wavelength requirement. This

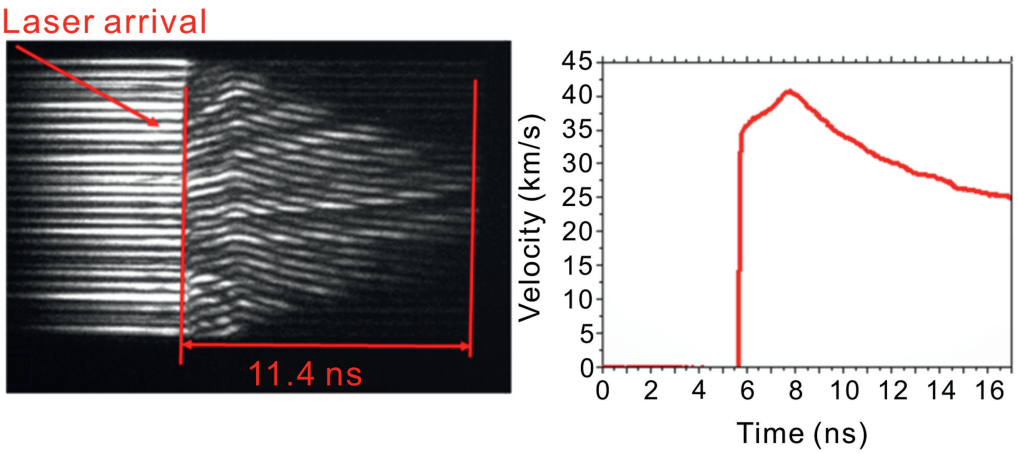

Fig. 9. Shock wave velocity of the quartz sample measured in SG-III with the VISAR laser source.

laser source can be connected to the original front-end system of SG-III to provide wavelength tuning capability for any beamline. The tuning capability is shown in Fig. 10.

3. Performance upgrade of SG-III

Besides the new functionalities added to SG-III, some performance upgrade is also important for physics experiment, such as improving the power balance capability and the beam smoothing capability. In the original design of SG-III, the power balance is required to be better than 10% for a flat-top pulse shape, while in the performance upgrade project, this requirement shifts to better than 5% in the peak of a shaped high contrast pulse. In the original design, only continuous phase plate (CPP) is used in SG-III, while the performance upgrade project asks to add smoothing by spectral dispersion (SSD) for all the 48 beamlines and polarization smoothing (PS) for the 16 inner beamlines.

3.1. Power balance

Power balance is a key laser performance index for ICF experiments, which is the premise for target pellet imploding

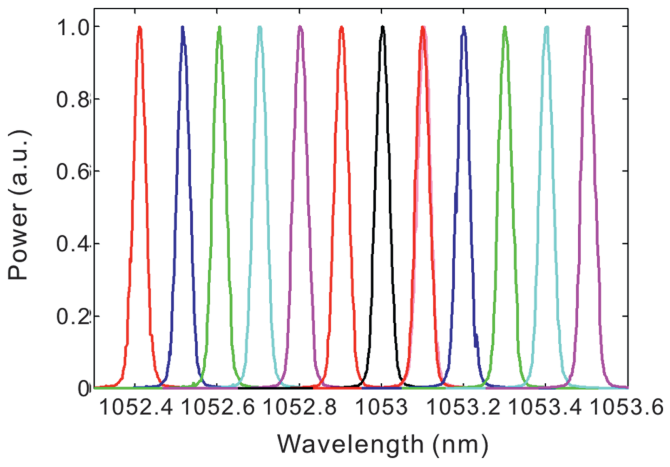

Fig. 10. Wavelength tuning capability in SG-III.

symmetrically. The index of power balance in fact reflects the driving laser power imbalance on the target at a given time. In most laser driven experiments, indirect driven method [20] is adopted by which the laser converts to X-ray radiation firstly, and then the X-ray drives the target pellet. During laser-X-ray conversion, the power imbalance is smoothed, so strict instantaneous laser power balance is not required in indirect drive ICF experiments. In NIF, the laser power balance is defined as the standard deviation of the individual quad power profiles relative to the average value of the power for a common pulse shape, boxcar averaged over 2 ns time interval [21]. At the end of NIC, NIF demonstrated its power balance capability could meet the requirement of an ignition-point design pulse shape, being 12% (RMS) in the picket, 20% (RMS) in the trough, and 3% (RMS) during the peak of the pulse [21]. For SG-III, its original laser power balance requirement is 10% for a 3 ns flat-top pulse. Since we still lack a common smoothing window specification for power balance in SG-III, we use both 500 ps and 2 ns smoothing windows to evaluate the power balance. In the autumn of 2015, SG-III demonstrated its power balance capability with all the 48 beamlines using a little bit complex pulse shape as shown in Fig. 11. The diagnostics here we used were a phototube with 80 ps rising edge and an oscilloscope with 8 GHz bandwidth. As the performance upgrade project started, the request for power balance is stricter as better than 5% in the peak of a shaped high contrast pulse. To achieve better power balance capability, three ways are pushed forward: developing the Laser Performance and Operation Simulation System (LPOSS), improving laser energy stability, and enhancing pulse shaping precision.

LPOSS is based on previous laser simulation code SG-99, while new functionalities are added, such as laser injection prediction, shooting simulation and safety analysis, history data analysis and laser performance evaluation. The most important functionality for power balance is the laser injection prediction. With 5 year's laser operation data, LPOSS can provide predicted injection laser energy and pulse shape, which can direct laser operation and shorten adjusting time. At the end of the performance upgrade project, with an LPOSS-

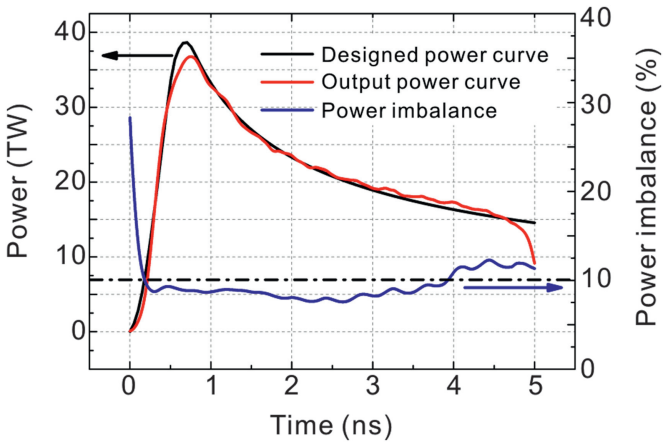

Fig. 11. Power balance capability of SG-III before performance upgrade project (boxcar averaged in 500 ps).

predicted laser injection, the shooting laser power derivation of each beamline from the required laser power curve is less than 10% even for a complex high-contrast laser pulse. LPOSS with the real optics information of each beamline can now significantly improve the shooting efficiency and works well in daily operation.

The basic physics model of LPOSS is the laser propagation and amplification model in gain medium as well as frequency conversion model in nonlinear crystal. It contains lots of parameters such as transmittivity of the optics, small gain and loss coefficient of the amplification medium, surface profile of optical components and so on, which have significant influence on the laser energy and pulse shape. Although the historical operation data contributes to the revision of the model parameters, to calculate the whole 48 laser injections according to the objective 3ω laser power curve in parallel is a large amount of calculation, which reduces the adjusting efficiency greatly. To improve the calculation efficiency, a simplified method with acceptable calculation precision is developed and Fig. 12 gives an example of this iteration process. For a required ignition pulse shape, LPOSS gives the injection laser power curve after 4 iterations, with which the difference between simulated and objective output laser power curve is less than 1%. Fig. 13 gives a comparison of an LPOSS-simulated

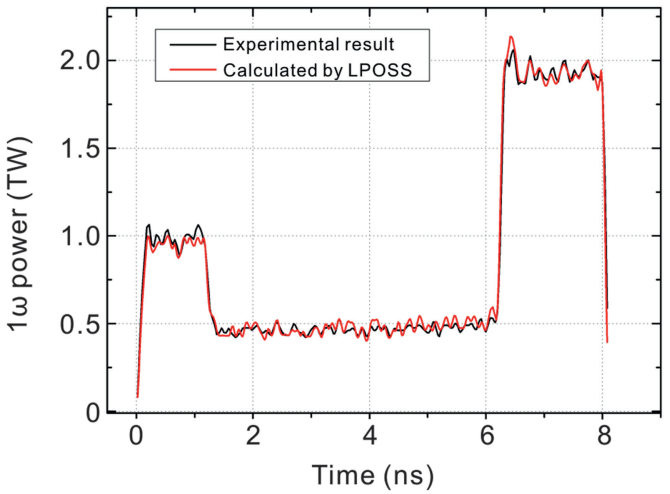

Fig. 13. Comparison of LPOSS calculated and experimental 1ω laser power curve.

8 ns 1ω laser pulse and the real shot result in one beamline of SG-III. According to the result, LPOSS can exactly simulate the laser propagation and amplification processes, which greatly improves the laser adjusting efficiency for the whole 48 beamlines.

Laser energy stability is the foundation of power balance. According to history operation data, the laser energy instability mainly comes from the front-end system and the preamplifier

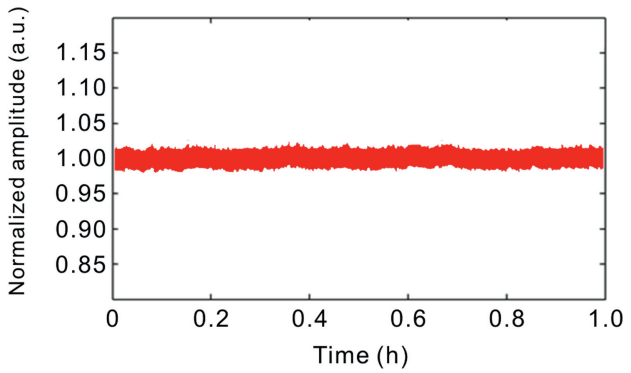

Fig. 14. Energy stability testing result in the front-end system of SG-III.

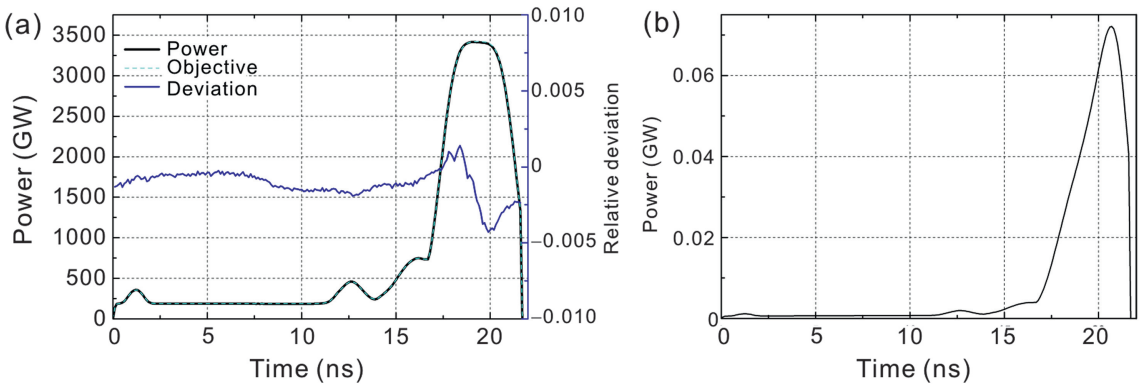

Fig. 12. (a) Calculated laser power curve by LPOSS after 4 iterations compared with the objective power curve; (b) Calculated injection laser power curve.

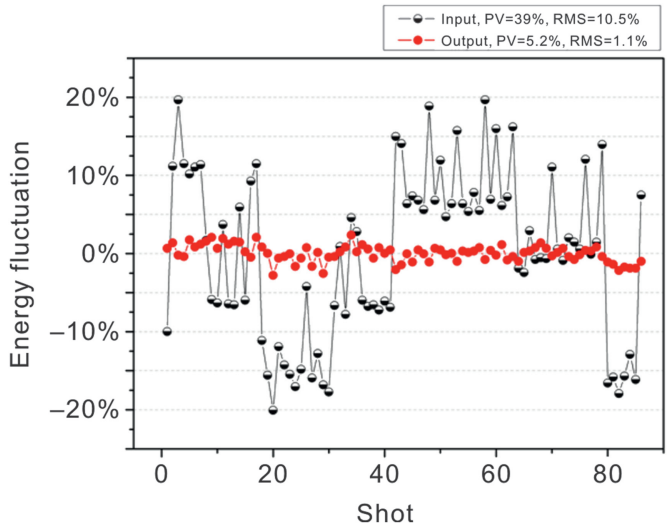

Fig. 15. Offline input and output energies in preamplifier system with active stabilizing method. Reproduced from Ref. [12].

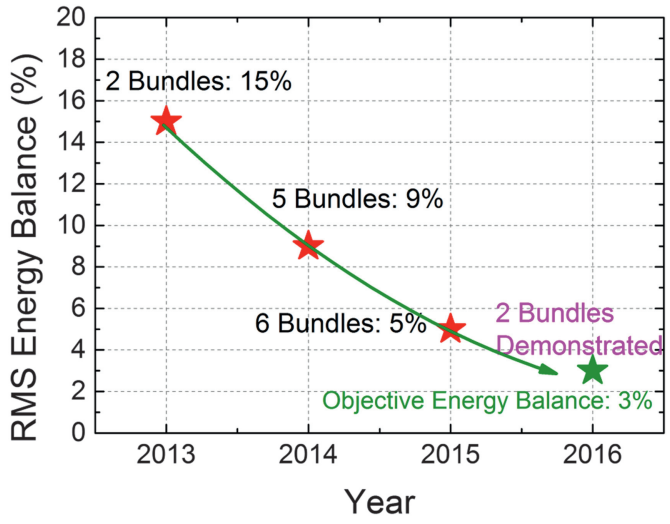

Fig. 16. Energy stabilizing progress in SG-III.

system. During the performance upgrade project, all the fiber elements that may induce energy instability had been checked carefully, some polarization fibers had been replaced by PZ fiber, and finally the output laser energy stability were kept in 5%–8% (PV) and less than 1% (RMS) [12]. Fig. 14 shows a testing result of one beamline in the front-end system of SG-III, and the energy stability in one hour is 5.02% (PV) and 0.58% (RMS). The laser pulse from the front-end system will inject into the preamplifier system and the pulse energy will be amplified nearly 10^9 times. Thus any instability from the front-end system will be amplified. Furthermore, the preamplifier system itself will bring new instabilities to the laser pulse, such as the fluctuation of the pump, improper state of the Pockels cell and so on. In performance upgrade project, besides carefully adjusting the working state of each active device in the pre-amplifier system and avoiding any electromagnetic interference, two technical methods are adopted to improve the laser energy stability. One is lengthening the pump duration from 400 μs to 700 μs, which effectively lowers the flash fluctuation of the xenon lamp. The other is adding a photoconductor in the preamplifier system which pre-detects the laser pulse energy and suppresses the energy instability through a Pockels cell. Fig. 15 gives the offline testing result of the preamplifier system with these technical methods. The instability of the input signals was adjusted artificially with a PV fluctuation of 39%, while the output PV value was suppressed to 5.2%. The good energy stabilizing result pushes these technical methods to be applied in SG-III. In fact, pursuing better laser energy stability accompanies with the engineering construction and performance upgrade of the SG-III laser facility. Fig. 16 shows this progress in the past few years.

To precisely tuning the physics process during implosion, it is essential to shape the laser pulse as accurate as possible. The only pulse shaping unit is the arbitrary waveform generator (AWG) locating at the front-end system (Tecktronix 7122B, temporal resolution 0.1 ns, number of addressable elements 60000). Thus proper feedbacks must be provided to correct the pulse shapes precisely and efficiently. A closed-loop pulse

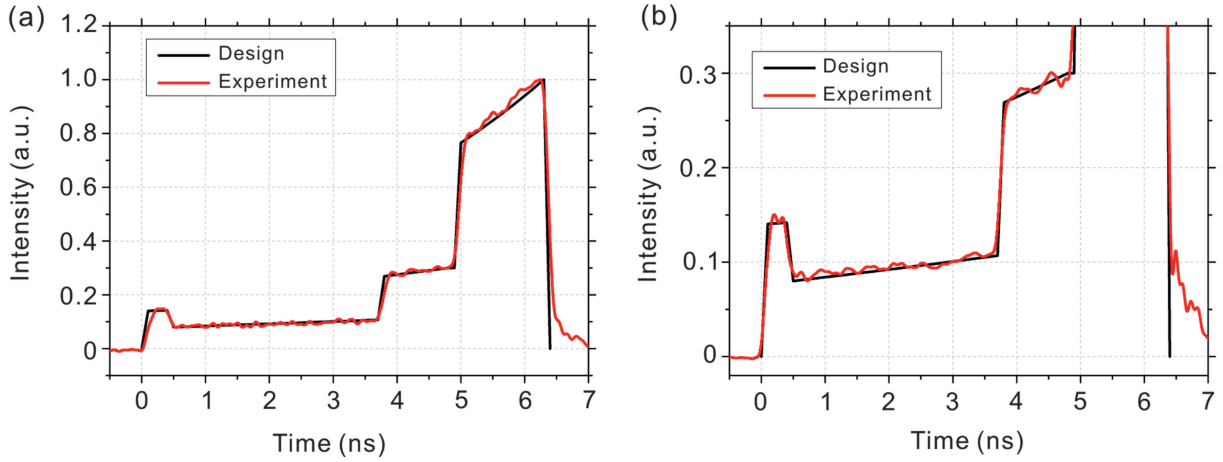

Fig. 17. Typical pulse shape at the repetitive amplifier of preamplifier system after the closed-loop pulse shape revision. Right figure is the detail of the lower section in the left figure.

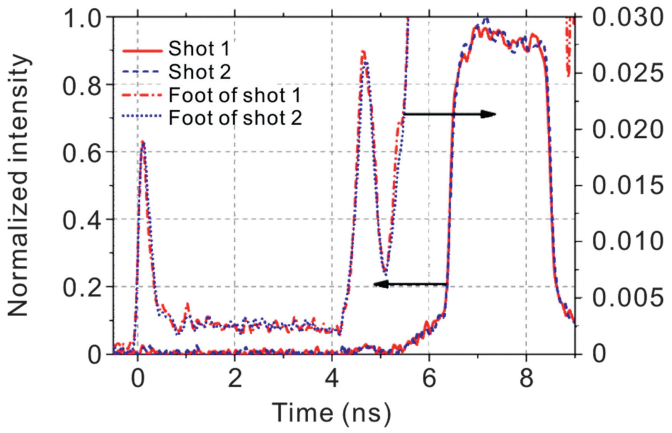

Fig. 18. Demonstration of SG-III's capability of pulse shaping and measurement for high pulse dynamic range. Reproduced from Ref. [22].

shaping sub-system is added to the front-end system, a pulse shape feedback point is set after the preamplifier system. When this sub-system is working, only the repetitive amplifier at 1 Hz is working, a 5-time-averaged pulse shape after the preamplifier is recorded by a computer which analyzes the pulse shape derivation from the designed one, and revises the driving voltage in AWG. This sub-system can correct the pulse shapes of 12 beamlines simultaneously and for each beamline, no more than 20 times of closed-loop revisions are made before the pulse shape meets the design requirement. Fig. 17 shows a typical pulse shape after the repetitive amplifier in the preamplifier system. This closed-loop pulse shaping sub-system only ensures the shaping accuracy in the repetitive amplifier section, while the final 3ω pulse shaping accuracy after pulse amplification and propagation depends on the simulation precision of the LPOSS. This whole pulse shaping process was demonstrated in the Beam Integrated Diagnostic System (BIDS) in 2015 [22]. One beamline of SG-III was redirected to the BIDS, and two main shots were made to test the pulse shaping capability and the measurement capability for high dynamic range. The result is shown in Fig. 18. A complex pulse shape with 9 ns pulse duration and 300:1 dynamic range was demonstrated with good repeatability. Meanwhile, the measurement capability for high dynamic range of 1000:1 has been demonstrated. A power divider was used to split the signal to two channels of the oscilloscope with splitting ratio of 1:1. This splitting ratio was demonstrated offline, and it was quite stable during the whole offline test, which is also proved by the reproducibility of the dynamic ranges of the pulse shapes in Fig. 18.

With the preparation of LPOSS, energy stability and pulse shaping capability, the testing for power balance was conducted with 16 beamlines from two middle ring bundles in June, 2016. The dynamic range of the pulse shape is about 160:1. Fig. 19 gives the total laser power curve compared with the requested

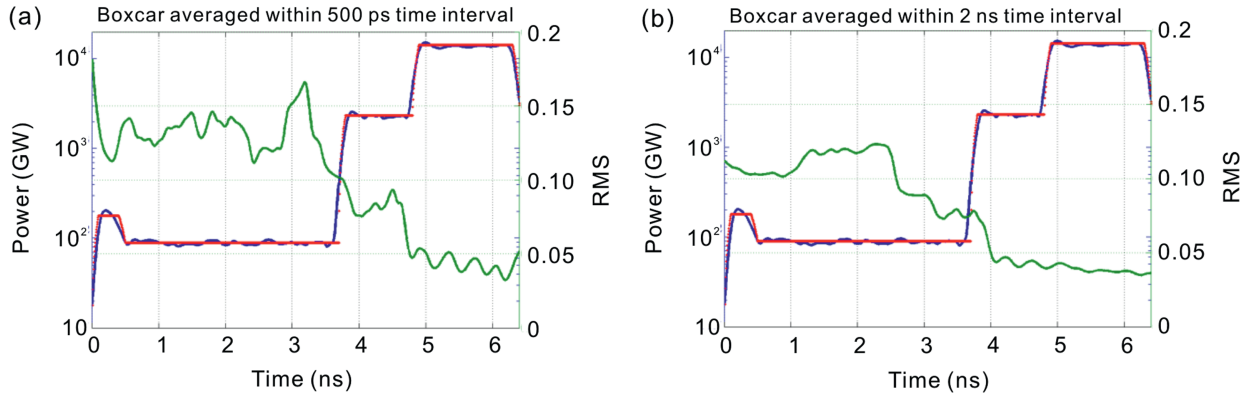

Fig. 19. Power balance testing result in SG-III with boxcar averaged in (a) 500 ps and (b) 2 ns. The dotted line is the objective power curve, the blue line is the experimental result and the green line is the power imbalance curve.

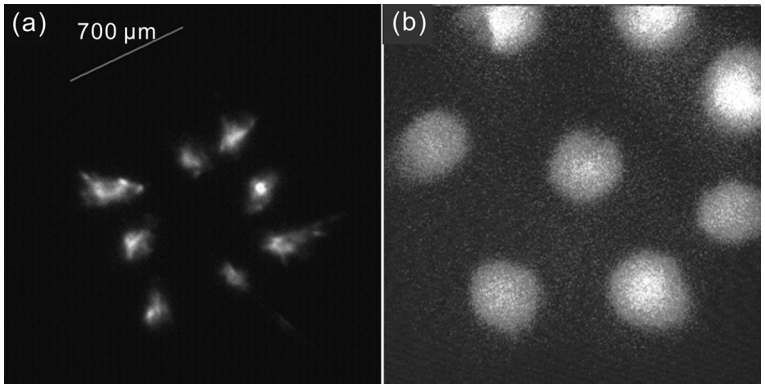

Fig. 20. Focal spot of the SG-III A6 bundle in 2012 before performance upgrade: (a) optical focal spot without CPP; (b) X-ray focal spot with CPP.

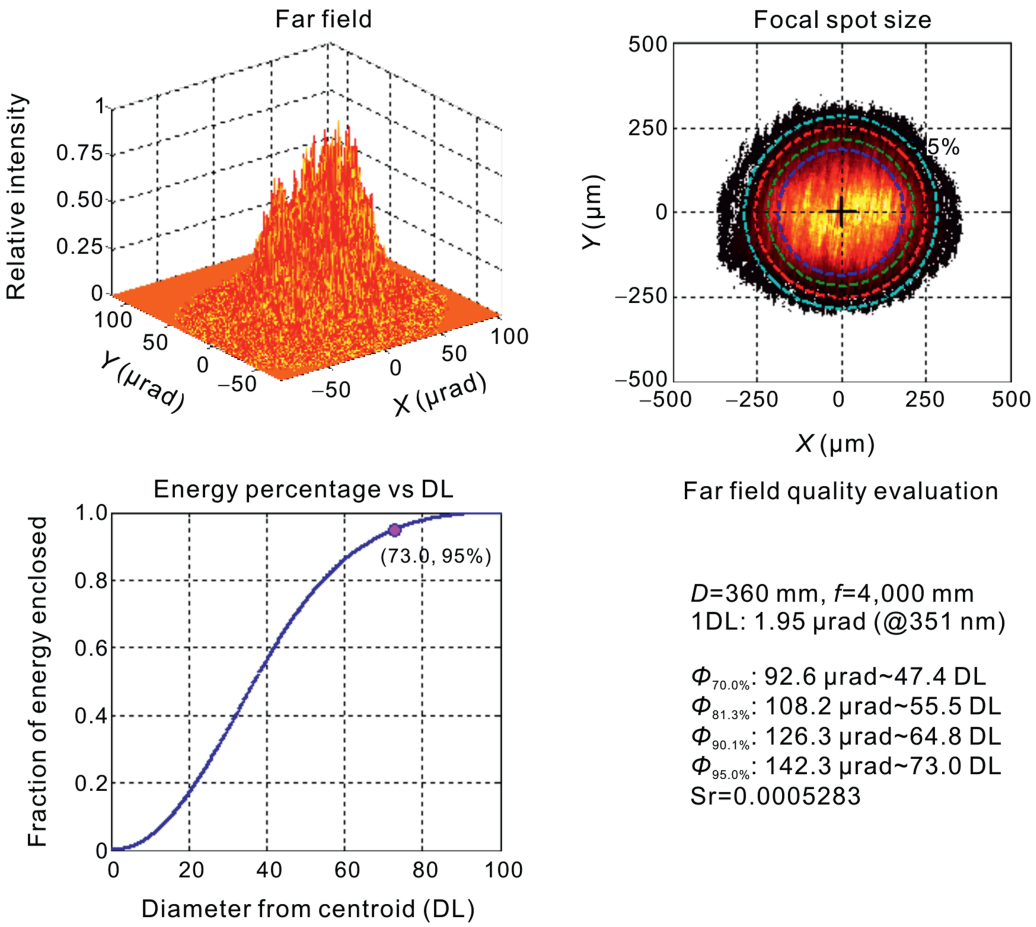

Fig. 21. The laser focal spot distribution with 500 μm CPP and SSD.

one and the power imbalance curve with 500 ps and 2 ns boxcar averaging respectively. In this shot, the power imbalance is about 4% in the peak and about 12% in the lower section before 3.7 ns. This result demonstrates that after the work in the performance upgrade project, SG-III now possesses good power balance capability, which can strongly support the ICF studies before achieving fusion ignition in China.

3.2. Beam smoothing

Beam smoothing is an effective way to suppress LPI instability so that it is a very important technical way for achieving fusion ignition. There are many technical methods for beam smoothing, however, those have been adopted in huge laser drivers only include CPP, SSD and PS [23–25]. In SG-III's original design, only CPP is considered for beam smoothing. Fig. 20 shows the focal spots with and without CPP of the A6 bundle lasers of SG-III in 2012 before performance upgrade. As the performance upgrade project started, SSD for all the 48 beamlines and PS for inner ring 16 beamlines were also required in SG-III.

For suppressing transverse SBS in large optics [26], a 2.488 GHz phase modulator has already been installed in the SG-III's front-end system which expands the laser spectral width to 0.15 nm. According to the requirement of SSD, another phase modulator with higher modulating frequency should be added after the first one. Here we add a 19.9 GHz phase modulator, with which the laser spectral width will be expanded to 0.3 nm. We use a 616 l/mm grating which leads to a designed speckle displacement of 1 diffraction limit and color cycle of 1. In the testing for SSD effect, main shot of 3 ns flat-top pulse was made with a 3ω energy of 1516 J. Fig. 21 shows the testing result of SSD. From the top view of

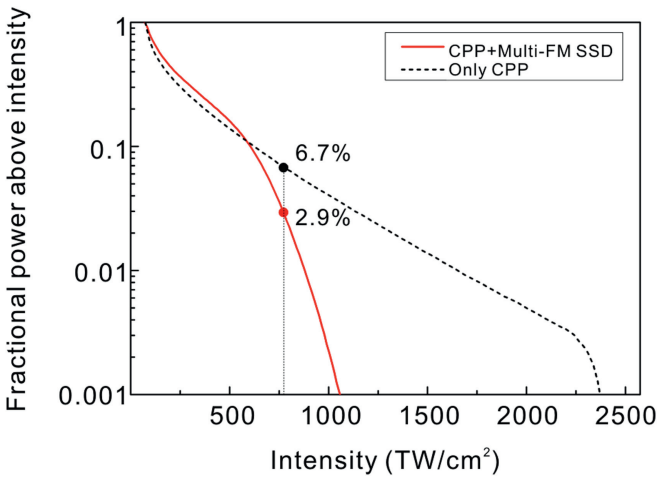

Fig. 22. FOPAI curve of the laser focal spot with only CPP and CPP + SSD respectively. Multi-FM SSD means two modulation frequencies of 2.488 GHz and 19.9 GHz.

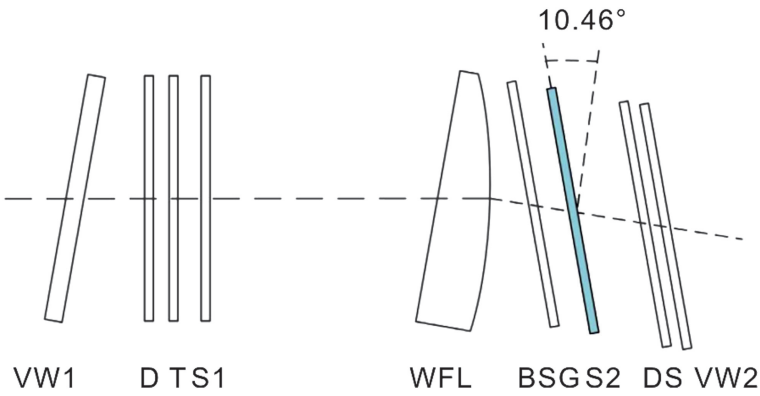

Fig. 23. Location (S2) of the KDP scrambler in the FOA of SG-III. VW: vacuum window, D: frequency doubler, T: frequency tripler, S: slot for optics, WFL: wedge focusing lens, BSG: beam sampling grating, DS: debris shield. Reproduced from Ref. [30].

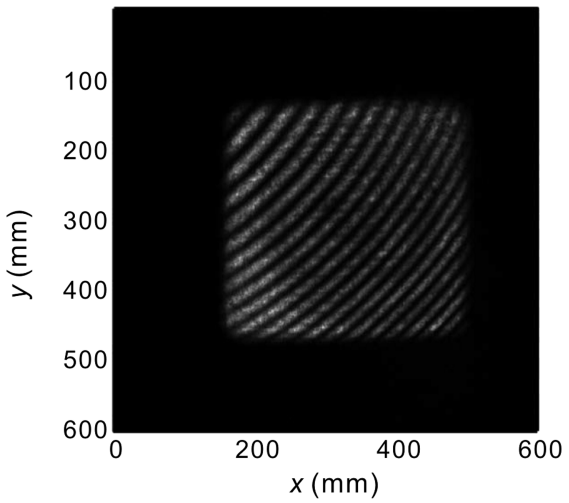

Fig. 24. Laser nearfield after the KDP scrambler and a polarization analyzer.

the focal spot, it is clear that the SSD works well and blurs the speckles in the focal spot in one dimension. One-dimensional SSD is adopted in SG-III, while the two-dimensional SSD technique has been tested in the U.S. [27] which can further smooth the focal spot for direct drive. Fig. 22 is the fraction of power above intensity (FOPAI) curve, from which we can clearly see the SSD smoothing effect. Now SSD can be applied to all the 48 laser beamlines of SG-III when needed.

PS is an instantaneous beam smoothing method that equally divides the laser near field to e- and o-polarized parts. These two parts slightly drift apart in the far field and overlap incoherently, thus smooth the focal spot by a theoretical factor of $1/\sqrt{2}$. For single beam smoothing, birefringent wedge can be used in the collimated part of the ultraviolet beam, such as in OMEGA and NOVA [13,28]. For NIF, its 2×2 FOA supports polarization combination of its sub laser beams [29]. In SG-III, we use a KDP scrambler in the convergent beam [30] as shown in Fig. 23. Since the scrambler in the convergent beam will divide the polarizations into isogyre patterns, with a polarization analyzer, we get a laser nearfield distribution as same as calculations (Fig. 24). The PS effect is shown in Figs. 25 and 26. With PS method, the speckles in the focal spot have been blurred obviously and the FOPAI curve declines apparently. After the performance upgrade project, SG-III can provide PS function for 16 beamlines. Since the KDP scramblers have a similar smoothing effect for vertically and horizontally polarized beamlines,

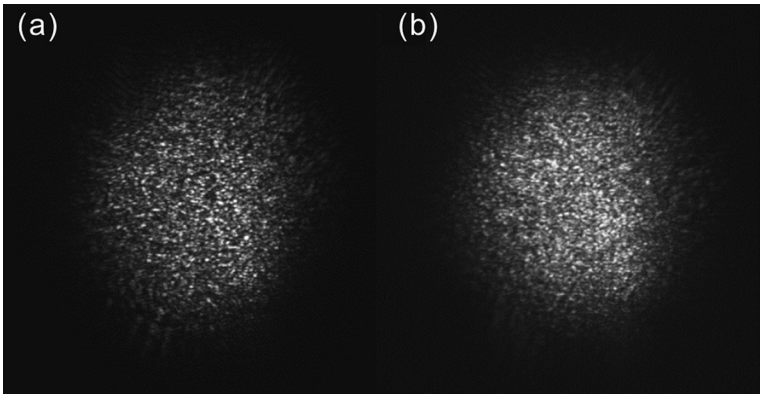

Fig. 25. Focal spots (a) without and (b) with PS in SG-III.

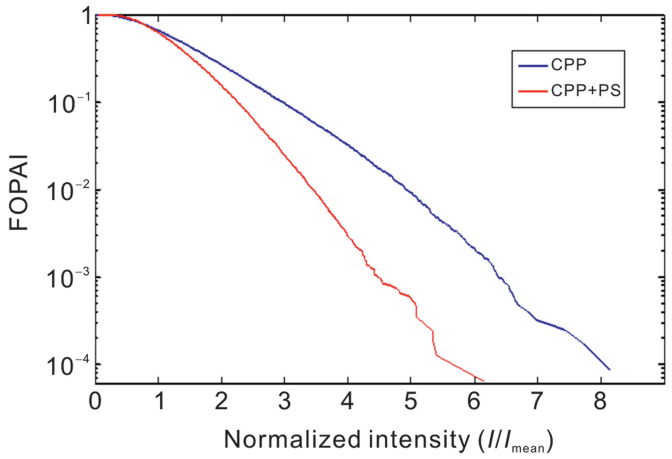

Fig. 26. FOPAI curve of PS effect.

they can be used in any beamline in SG-III. Details of PS in SG-III can be obtained from Ref. [30].

4. Conclusion

In the past 2 years, the SG-III laser facility extended its functionalities as well as upgrading some intrinsic capabilities, such as power balance capability and beam smoothing capability. After the upgrade project, SG-III now possesses much more confidence for precise ICF physics experiments. As the largest ICF research platform in China and the only 100 kJ-level laser driver around the world, SG-III is now prepared for precise ICF physics experiments and with high expectations to provide deeper understanding of hohlraum physics processes before the laser driving energy reaches ignition level. It is believed that experiments in the SG-III laser facility will be of guiding significance to the design of ignition level laser driver and experiment.

Acknowledgement

This work is supported by the SG-III performance upgrade project.

References

[1] M. Dunne, Laser Inertial Fusion Energy (LIFE) – a path to US energy independence, in: Annual Meeting of the Southern States Energy Board, 2012.
[2] J.D. Lindl, P. Amendt, R.L. Berger, S.G. Glendinning, S.H. Glenzer, et al., The physics basis for ignition using indirect-drive targets on the National Ignition Facility, Phys. Plasmas 11 (2) (2004) 339–491.
[3] M.D. Rosen, J.D. Lindl, J.D. Kilkenny, Recent results on Nova, J. Fusion Energy 13 (2–3) (1994) 155–166.
[4] T.R. Boehly, R.S. Craxton, T.H. Hinterman, J.H. Kelly, T.J. Kessler, et al., The upgrade to the OMEGA laser system, Rev. Sci. Instrum. 88 (l) (1995) 506–510.
[5] C.A. Haynam, P.J. Wegner, J.M. Auerbach, M.W. Bowers, S.N. Dixit, et al., National Ignition Facility laser performance status, Appl. Opt. 46 (16) (2007) 3276–3303.
[6] National Ignition Campaign Execution Plan, UCRL-AR-213718, NIF-0111975-AA, Rev. 0, June 2005.
[7] National Ignition Campaign Program Completion Report, LLNL-TR-637982, September 30, 2012.
[8] J. Ebradt, J.M. Chaput, LMJ on its way to fusion, J. Phys. Conf. Ser. 244 (2010) 032017.
[9] X.T. He, W.Y. Zhang, C.F. Ye, Inertial fusion energy research progress in China, in: 6th Symposium on Current Trends in International Fusion Research: A Review, Washington, D.C., USA, 7–11 March 2005.
[10] Z.Q. Lin, X.M. Deng, D.Y. Fan, S.J. Wang, S.H. Chen, et al., SG-II laser elementary research and precision SG-II program, Fusion Eng. Des. 44 (1999) 61–66.
[11] P. Li, F. Jing, D.S. Wu, R.C. Zhao, H. Li, et al., Power balance on the SG-III prototype facility, Proc. SPIE 8433 (2012) 843317.
[12] W.G. Zheng, X.F. Wei, Q.H. Zhu, F. Jing, D. Hu, et al., Laser performance of the SG-III laser facility, High Power Laser Sci. Eng. 4 (2016) e21.
[13] J.D. Moody, B.J. MacGowan, J.E. Rothenberg, R.L. Berger, L. Divol, et al., Backscatter reduction using combined spatial, temporal, and polarization beam smoothing in a long-scale-length laser plasma, Phys. Rev. Lett. 86 (13) (2001) 2810–2813.
[14] G.A. Kyrala, A. Seifter, J.L. Kline, S.R. Goldman, S.H. Batha, et al., Tuning indirect-drive implosions using cone power balance, Phys. Plasmas 18 (7) (2011) 072703.
[15] C.K. Li, F.H. Seguin, J.A. Frenje, S.R. Goldman, S.H. Batha, et al., Effects of nonuniform illumination on implosion asymmetry in direct-drive inertial confinement fusion, Phys. Rev. Lett. 92 (20) (2004) 205001.
[16] J. Fuchs, C. Labaune, S. Depierreux, H.A. Baldis, A. Michard, et al., Modification of spatial and temporal gains of stimulated Brillouin and Raman scattering by polarization smoothing, Phys. Rev. Lett. 84 (14) (2000) 3089–3092.
[17] R.M. Malone, J.R. Bower, D.K. Bradley, T.W. Tunnell, Imaging VISAR diagnostic for the National Ignition Facility (NIF), in: SPIE High-speed Photography and Photonics Conference Alexandria, VA, United States, UCRL-CONF-206587, 2004.
[18] R. Zhang, M.Z. Li, J.J. Wang, W. Duan, F. Wang, et al., Experimental research on an arbitrary pulse generation system for imaging VISAR, Opt. Laser Technol. 43 (2011) 179–182.
[19] S.H. Glenzer, B.J. Macgowan, P. Michel, N.B. Meezan, L.J. Suter, et al., Symmetric inertial confinement fusion implosions at ultra-high laser energies, Science 327 (5970) (2010) 1228–1231.
[20] J. Lindl, Development of the indirect-drive approach to inertial confinement fusion and the target physics basis for ignition and gain, Phys. Plasmas 2 (1995) 3933.
[21] M.L. Spaeth, K.R. Manes, M. Bowers, P. Celliers, J.M.D. Nicola, et al., National Ignition Facility laser system performance, Fusion Sci. Technol. 69 (2016) 366–394.
[22] D.X. Hu, J. Dong, D.P. Xu, X. Huang, W. Zhou, et al., Generation and measurement of complex laser pulse shapes in the SG-III laser facility, Chin. Opt. Lett. 13 (4) (2015) 041406.
[23] J. Néauport, X. Ribeyre, J. Daurios, D. Valla, M. Lavergne, et al., Design and optical characterization of a large continuous phase plate for laser integration line and laser megajoule facilities, Appl. Opt. 42 (23) (2003) 77–82.
[24] S. Skupsky, R.W. Short, T. Kessler, R.S. Craxton, Improved laser-beam uniformity using the angular dispersion of frequency-modulated light, J. Appl. Phys. 66 (34) (1989) 56–62.
[25] J.E. Rothenberg, Polarization beam smoothing for inertial confinement fusion, J. Appl. Phys. 87 (2000) 3654–3662.
[26] J.R. Murray, J. Ray Smith, R.B. Ehrlich, D.T. Kyrazis, C.E. Thompson, et al., Experimental observation and suppression of transverse stimulated Brillouin scattering in large optical components, J. Opt. Soc. Am. B 6 (12) (1989) 2402–2411.
[27] S.P. Regan, J.A. Marozas, R.S. Craxton, J.H. Kelly, W.R. Donaldson, et al., Performance of 1-THz-bandwidth, two-

dimensional smoothing by spectral dispersion and polarization smoothing of high-power, solid-state laser beams, J. Opt. Soc. Am. B 22 (5) (2005) 998−1002.

[28] T.R. Boehly, V.A. Smalyuk, D.D. Meyerhofer, J.P. Knauer, D.K. Bradley, et al., Reduction of laser imprinting using polarization smoothing on a solid-state fusion laser, J. Appl. Phys. 85 (1999) 3444−3662.

[29] S.N. Dixit, D. Munro, J.R. Murray, M. Nostrand, P.J. Wegner, et al., Polarization Smoothing on the National Ignition Facility, UCRL-PROC-215251, Inertial Fusion Science and Applications, 2005.

[30] X.X. Huang, H.T. Jia, W. Zhou, F. Zhang, H. Guo, et al., Experimental demonstration of polarization smoothing in a convergent beam, Appl. Opt. 54 (33) (2015) 9786−9790.